PRODUCTIVITY IMPROVEMENT OF AUTOMOTIVE ROD FORMING PROCESS BY SIMULTANEOUS OPERATION USING FE SIMULATION

Harshal Ashok Chavan, Dhiraj Devrao Deshmukh

MET's Institute of Engineering, Bhujbal Knowledge City, Nashik, SPPU, Pune- 422003, India

Corresponding author: Harshal A. Chavan, chavanharshal@gmail.com

Abstract: Metal forming processes are the backbone of modern manufacturing processes. Connecting rods are used in automotive seats to connect recliners and achieve forward/backward movement of automobile front seats. Individual grooving, flatting and serration tools were used previously, which taking too much time for loading new die every time. The main objective of the work presented in this paper is to design a tool for simultaneous operation and simulate forming process for increasing the productivity through process optimization. Various elements of the tool are developed by calculating forming forces. Further, the forming process is simulated using finite element simulation before building of combination tool. The simulation results obtained for the stress and deformation state are discussed. The designed combination tool is fabricated and implemented successfully in one of the leading automotive component manufacturing industry. Results found are acceptable with fewer defective rods and enhancement in productivity with decrease in lead time compared to the earlier tool.

Key words: Finite element Simulation, Metal forming, Combination tool, Forming force distribution, Productivity improvement.

1. INTRODUCTION

The work is focused on designing a new combination tool and simulating the forming process to execute three processes simultanously on a rod. The recliners of driver and co driver seats are connected by the rod to accomplish movement as shown in Figure 1. Total three operations are carried out at one end and two operations at other end of the rod.

The work is intended to develop a combination tool for first three operations as grooving, flatting and serration in the sequence. Use of computer-aided engineering is very important in designing and developing a forming tool with lesser time and cost [1]. It was proven that combination tool design is optimal design, as it optimizes the process. Diamentional precision of the tool assembly should continue for the entire functioning life of the combination tool [2].

Use of forming simulation is advantages over the trial tools, as it leads to a significant reduction in both cost and time [3, 4]. Simulation of forming process has exposed new prospects due to continuous enhancement in FE simulations [5]. Simulation is important in designing metal forming process, not only for material properties and frictional conditions but also for geometric representations and computational time [6]. Simulation greatly improves the understanding of mechanics by visualizing the deformation and stress in component. FE simulation is more proficient in resolving compound design and manufacturing concerns in metal forming [7]. The accuracy of the simulation results depends on several factors: the type of finite element, the discretization of the analyzed object, the solving algorithm, etc. It helps to improve the quality with minimum product development time. The application of modelling and process simulation is highly important in metal forming, hence it must be applied at the time of design phase only. FE simulation of the complete forming process is used to gain the information about forming sequences followed for obtaining the final shape of the component according to the drawing provided by the customer.

Fig. 1. Actual application of connecting rod

2. ANALYTICAL DESIGN OF COMBINATION TOOL

A circular pipe of AISI /SAE 1010 material is required to convert in a square from one end. Formerly first operation was grooving finished independently on the rod by altering the circular shape into a rectangular shape followed by flatting and serration [8, 9]. The shape of the product is illustrated in Figure 2.

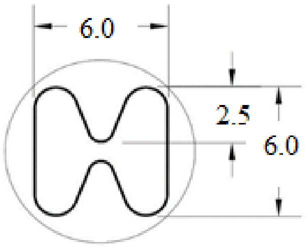

Fig. 2. Final required shape of connecting rod

To complete above operations, different dies were mounted on the same press according to the operation being carried out. It was very time-consuming concern to change the die after each operation for the defined batch size, which causes reduction in productivity. Also, previous conventional tools were causes different defects while manufacturing connecting rod. Defects were resulted as difficulties in assembly at the customer end and fatigue for the operator at rework station, this rework increases the overall lead time. The work is carried out with the replacment of three different dies in a single die, thus optimize the process.
Components of combination tool considering OHNS (Hardened at 62 HRC) material are designed stage-wise as follows [10].

2.1 Process -I (Grooving)

Figure 3 illustrates details about the first operation that is grooving [11]. Tool is designed based on rigidity theory and accuracy of component.

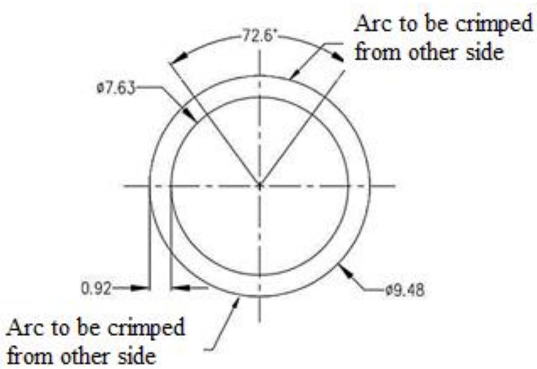

Fig. 3. Arc lengths to be crimped

2.1.1 Groove punch

The groove forming punch is modelled by component reference which has 2.7 mm thickness as shown in Figure 4 (a) and 4 (b), 0.5 mm thickness slot is kept to fix a punch in holder.
By 2D CAD model and geometry, exactly 2.7 mm thickness is faced an arc of 2.9 mm. Therefore actual thickness of punch,

t = 2.9-0.2 (0.1 clearance per side)
= 2.7

Thickness of punch = 2.7 mm
The groove forming punch of 2.7 mm thickness is modeled by component with reference to Figure 4(a) and 4(b) and slot of thickness 0.5 mm is provided for fixing the punch with punch holder.

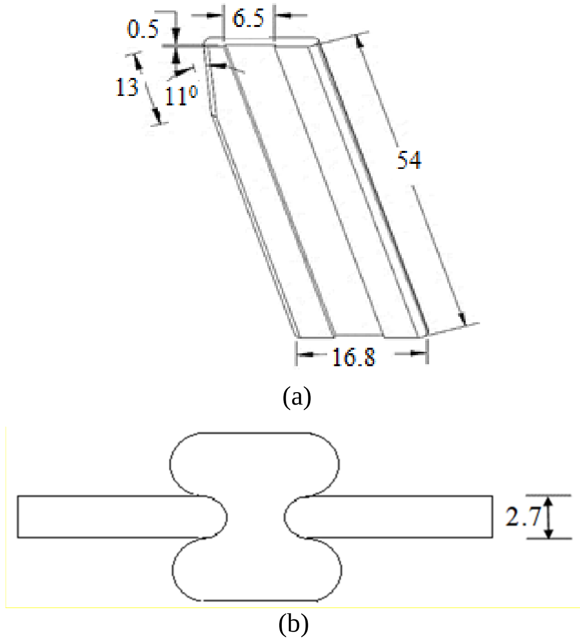

Fig. 4. (a) Forming Punch required for grooving; (b) Actual thickness of grooving punch

Force necessary for bending over the length as illustrated in Figure 5, is given by equation (equation (1)) [12].

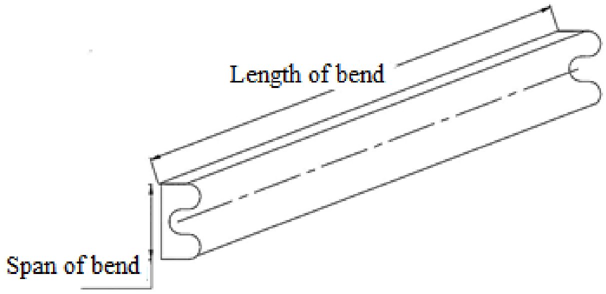

Fig. 5. Actual span & length of bend

$$F_b = \frac{K\,L\,S\,t^2}{W} \tag{1}$$

Bending force,

$$F_b = 4797.91\,N$$

From both sides total force required by groove punch is,

$$F = 9595.82\,N$$

Stress during compressive on punch,

$$\sigma_{Compressive} = \frac{F}{A} \quad (2)$$

$$\sigma_{Compressive} = 32.90\,Mpa$$

Where,
K = 1.33 constant factor for V bending
L = 54 mm (Length along the axis of bend)
S = 494.85 Mpa (Ultimate tensile strength of material)
t = 0.9 mm (Thickness)
W= 6 mm (Span of bend)
A= Striking area of punch in mm^2
F= Force applied by punch in N

2.1.2 Holder for punch during grooving

Geometric features (thickness, width, height) are created as per part drawing as illustrated in Figure 6.
Force acting on grooving punch holder plate is same as of bending force.
Stress induce in the component,

$$\sigma_{Compressive} = \frac{F}{A} = \frac{4797.91}{54 \times 2.8}$$

$$\sigma_{Compressive} = 31.73\,Mpa$$

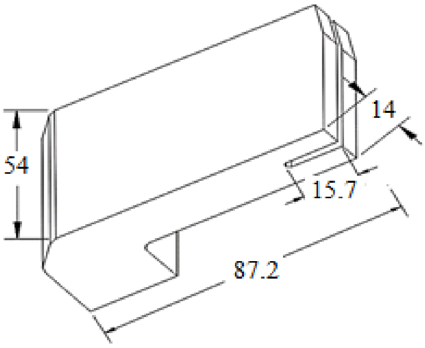

Fig. 6. Groove punch holder

Figure 7 illustrates the vertical force acting in the slot due to punch, which responsible for expanding the slot of the grooving punch holder. Assume the portion of the slot is to be a cantilever support.

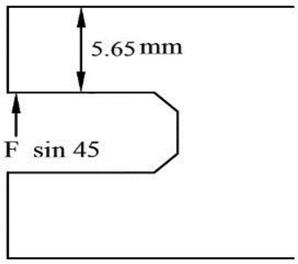

Fig. 7. Vertical force acting on punch holder

By Maculay's method, [13].

$$\delta_{max} = 0.031\,mm$$

Obtained deflection is within the tolerance limit.

2.1.3 Punch designed for flatting

From top and bottom same amount of force will be required as that of bending force. Hence effective force necessary from both side of punch is same as that of total grooving force.

2.1.4 Cam

It is a vertical member as shown in Figure 8, which exert the force from vertical to horizontal direction at follower (groove punch holder). Total deflection produced is 0.0032 mm in the cam due to 4797.91 N load transferred by cam (acting as cantilever to cam holder plate) to punch holder.

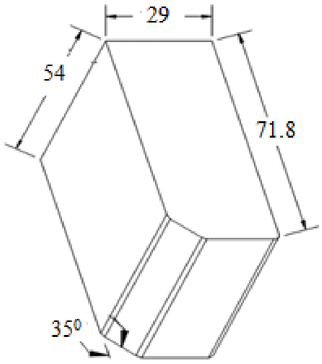

Fig. 8 Vertical CAM to exert force

2.1.5 Cam block guide plate

Horizontal force along with vertical force are exerted on guide plate. Deflection (δ_{max}) occurred is 0.0085 mm at plate due to horizontal force of 4797.91 N exerted to the cam considering cantilever support which is within the tolerance limit of the component. As the guide plate is simply supported member in the structure, maximum bending of the plate calculated under a vertical force of 4797.91 N is 0.15 mm. To limit the deflection of the plate within component tolerance limit, 24 mm thickness standard plate is added which acts as back plate for follower support block. Deflection δ_{max} = 0.018 mm is obtained after addition of this plate.

2.1.6 Spring calculation

Force produced by spring to bend from top equals to force required during forming is 4797.91 N. These springs are used to lock the rod from top in the course of action stroke. Total 12 parallel springs are used in vertical direction, so force necessary to generate by each spring is 399.80 N. For the revere stroke of follower total 2 springs are used in horizontal direction. Force required is 95.95 N to produce by each spring for the reversal of follower.

2.2 Process -II (Flatting)

The second process is flatting, that is carried out on the rod from vertical as well as horizontal sides. Flat punches are used in horizontal direction to obtain square shape of the component. Punches in vertical direction remains same as in first stage. Overall force acting on the component is same in all direction, so design of the components is same as in first stage.

2.3 Process -III (Serration)

Total 40 serration marks (6 mm x 0.2 mm) are protruded on component in third stage. Operation executed only at top and bottom surface. In this operation, serration punches are used at top and bottom for vertical stroke and flat punches for horizontal stroke remain same as that in second stage. Same material is used for all the punches used in combination tool.

The force required for serration for one side is,

S_{ut} of SAE 1010 = 494.85 Mpa

Force = S_{ut} x A

= 494.85 x 0.2 x 6

= 593.82 N

No. of serration marks = 40 (Nos.)

Force from one side = 23752.8 N

Force total from both side = 47505.6 N.

Total horizontal force required from both flat punches is 9595.82 N. Force required from all the sides in third stage is 57101.42 N i.e. (47505.6 N+ 9595.82 N).

3. SIMULATION OF THE FORMING PROCESS USING COMBINATION TOOL

It became more difficult when a single combination tool is required to be designed for performing more than one operation in single stroke of press due to complex part profiles and component material formability characteristics. Before developing the actual tool, mistakes can be avoided by performing the simulation of forming process [14]. To perform the finite element simulation of forming process using combination tool, LS-Dyna is used in the present investigation. Total 3 to 4 iterations are carried out as per the final required geometry of the component. Various types of defects occurred in previous forming process are also checked through FE simulation. Formability of the component can be predicted by FE simulation, which reduces the overall time and cost for the development of new tool [15].

3.1 Sequence of operation in simulation process

The designed combination tool is modelled with assembly of all components in new combination tool using Pro-E Wildfire 5.0 as shown in Figure 9 [16].

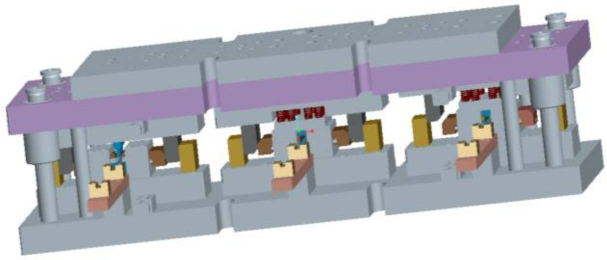

Fig. 9. New combination tool

Hypermesh version 14.0 is used for meshing the tool surface and component. Mid surface shell mesh is done on the component. Since thickness to length ratio of the component is very low, it is preferable to extract the mid-surface of the part, perform shell mesh on mid surface and assign the required thickness to it. For tools, since it is un-deformable only outer surfaces of the tools (which comes in contact with the part) are considered for the simulation and their outer surfaces are shell meshed and assigned RIGID (un-deformable properties) for FE calculation simplification. Process Sequence of simulation is carried out for the said work is as shown in Figure 10 [17].

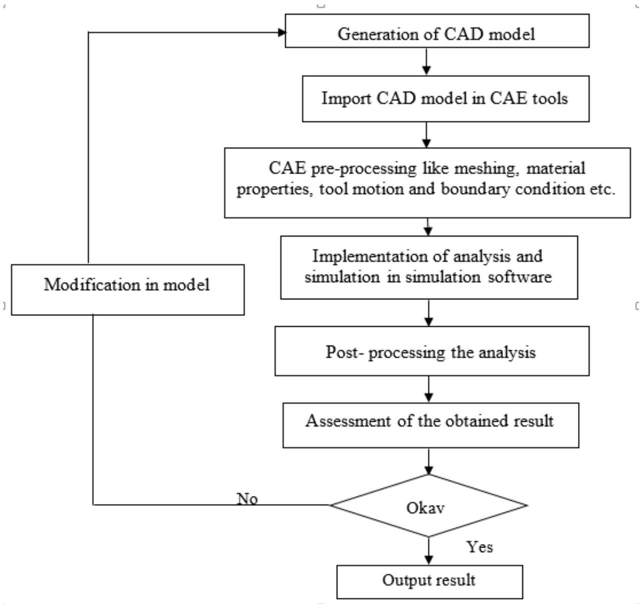

Fig. 10. Simulation process sequence

- Import CAD data of tool and part in Hypermesh.
- Extract mid-surface of the part and outer surface of tools.
- Perform 2D shell mesh on the part.
- Assign material properties, loads and boundary application, tool motion, surface to surface contact and dynamic friction coefficient to part and tools.
- Export the LS-Dyna solver input file.
- Submit the analysis job run in LS-Dyna input console.
- Post process the LS-Dyna analysis output files in Hyper-view and Hyper-graph to get the required deformation, stress, strain and force plots and graphs.

3.2 Material properties

For part- SAE 1010 used (MATERIAL CARD MAT24) to define a material which is elastic plastic material type in LS-Dyna to model the behavior of part under the action of deformation tool.

Tools- OHNS material (MATERIAL CARD MAT20) which is rigid un-deformable material type in LS-Dyna to model un-deformable components [18]. The material properties for MAT 24 are: Young's modulus 2.1×10^5 Mpa, Poisson's ratio= 0.3 and Yield strength=410 Mpa and for MAT 20 are Young's modulus 1.72×10^5 Mpa, Poisson's ratio= 0.3 and Yield strength=2150 Mpa are provided as mechanical characteristics of the component material.

3.3 Mesh information

In this forming analysis stage, a primarily hollow circular rod is located in between the grooving tool, generally come up with the die, punch, and blank holder. A small change in one region creates change in another region, hence deals in sheet metal forming processes are so intricate and those relations are nonlinear. Primarily, the sheet is discretized into finite elements of mesh and only outer surface of tools are included in FE model. 2D shell mesh is carried out on part mid surface with an average element size of 0.15 mm (since it is deformable very fine mesh is required to capture the deformation pattern of part accurately). Outer surfaces of tools are 2D shell meshed with average element size of 0.3 mm (since they un-deformable coarser element size can be used to reduce the analysis run time) as shown in Figure 11. In first stage, two movable grooving tools and two flat rigid tools are used in simulation having total 139006 elements and 139949 nodes. In second stage two flat moving tools and two flat rigid tools are used in simulation having total 149026 elements and 161788 nodes. In third stage two moving serration tools and two flat rigid tools are used in simulation having total 157246 elements and 184627 nodes.

3.4 Loading & boundary condition

Fixation of fixed tools is defined by suitable option in MAT_20 card (material card) for constraints [18]. For stage 1 *BOUNDARY_PRESCRIBED_MOTION is defined to give a displacement of 2.9 mm to the grooving tool at speed of 0.29 mm/ms (velocity is defined by load curve). Load curve ID (LCID) is changed by 3 to 4 iterations for every step to obtain the desired deformed shape of component. Curve ID or function ID is to describe motion value versus time. For stage 2*BOUNDARY_PRESCRIBED_MOTION is defined to give a displacement of 1.7 mm to the flatting tool at speed of 0.17 mm/ms. For stage 3 *BOUNDARY_PRESCRIBED_MOTION is defined to give a displacement of 0.2 mm to the serration tool at speed of 0.04 mm/ms as shown in Figure 12.

3.5 Stress-strain observed

Theoretical simulation approaches are centered mostly on elementary plasticity theory for pre-calculation of forming forces and rough calculation of stresses. There must be different stress conditions and high sufficient plastic strain present in the formed part to permit the differences to have a conclusion [19]. Maximum values of Von Mises stress are observed at contact points only, as it is the region where the utmost forces are developed [20].

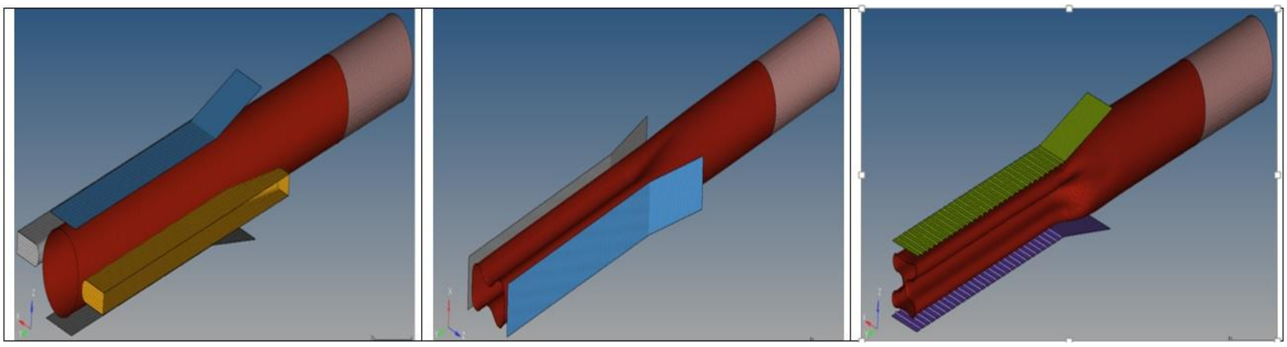

Fig. 11. Stage wise mesh information

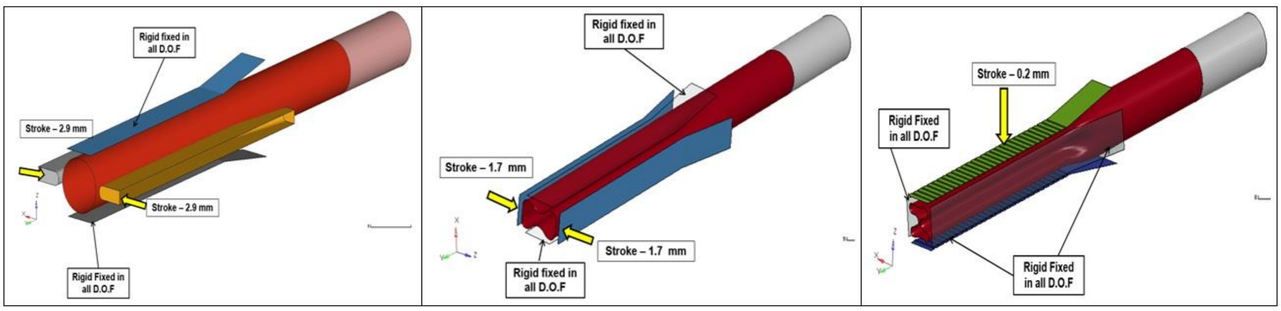

Fig. 12. Stage wise loading and boundary condition

Stage wise stress-strain plot obtained during simulation is shown in Figure 13(a) and 13(b). Von Mises stresses and maximum plastic strain at different operating conditions are plotted. Stress-strain obtained after each operation depends on the required force to achieve given shape of the component. After completion of the first operation, the component is subjected to flatting operation, for the same output shape of the first operation treated as input shape for the second operation. After completion of the second operation, the component is subjected to serration operation, for the same output shape of the second operation treated as input shape for the third operation where serration marks are protruded on the component. Average element size of 0.15 mm is selected for the component. As tool will remain un-deformable, coarser element size of 0.30 mm can be used to reduce the total analysis run time [21].

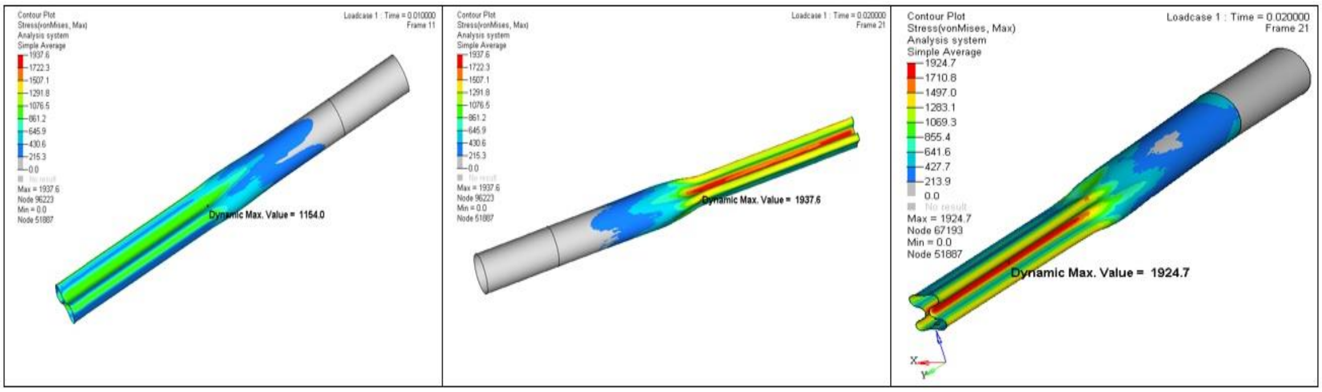

(a)

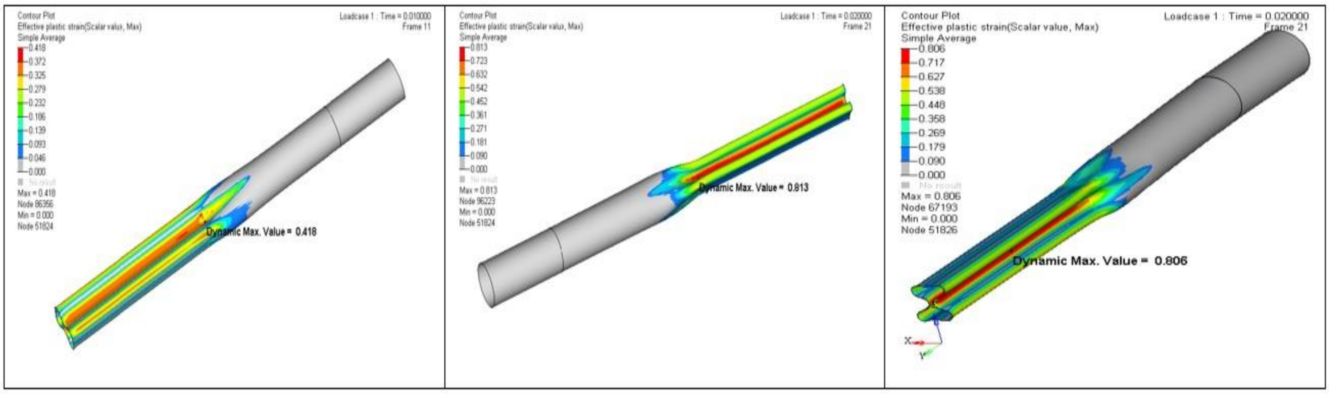

(b)

Fig. 13. (a) Stress distribution plot for all stages; (b) Strain distribution plot for all stages

4. FORMING FORCE FOR COMBINATION TOOL

Sometimes there is possibility of obtaining inaccurate forming force by the theoretical calculations, so it can be compare with the results obtained by simulation. Based on the geometric dimensions of the component, restraining force is calculated. The required forming forces in various operations are calculated analytically and compared with the FE simulation result. Difference between the analytically calculated values and obtained values of force by simulation are appended in Table 1.This force should be high enough to withstand the first forming of the component. Force required for all the operations are calculated analytically by designing various component of the combination tool. Force in first stage and second stage is equal as per analytical calculation. The simulation was done with prescribed tool motions, since the forces were unknown. The limiting forces designed for tool geometry are more accurate, as the contact between the tool and the component simulated in forming analysis as the component actually deforms when it passes through the working tool.

Table 1. Comparison of the obtained force

Stage No.	Operation	Force calculated analytically (N)	Force obtained by simulation (N)
1	Grooving	19191.64	19428.5
2	Flatting	19191.64	19604.5
3	Serration	57101.42	56658.3

4.1 Deformation observed in simulation

Stage-wise deformation of the component is visualised in simulation [22]. Deformed shape obtained after the first stage (grooving) on the circular pipe is the input for second stage operation. In second stage flatting of the component takes place with a flat tool from all the four side. In third stage, the linear serration are marked on the flat surface of the component for gripping purpose. This operation is consist of two flat tools and two serration tool. Deformation obtained after each stage is as shown in Figure 14.

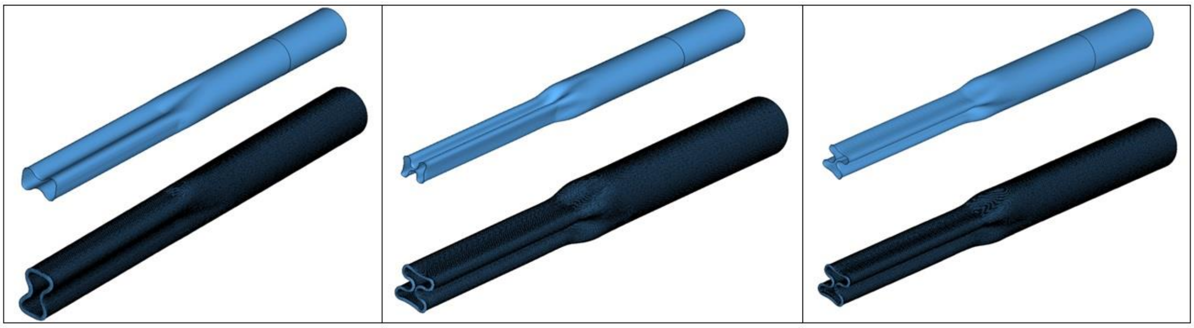

Fig. 14. Deformation observed after each stage

4.2 Force obtained by simulation

Maximum forces required in first, second and third stage with respect to time obtained by simulation are 19428.5 N, 19604.5 N and 56658.3 N respectively as shown in Figure 15.

The comparison of the finite element simulation results with the experiments has shown good accuracy to the analytical method. Additional work is essential to improve the analytical approach by the consideration of elastic deformation and three-dimensional stress state for the plastic deformation. As seen from the result, theoretical calculations for forming forces are very close to the force obtained by the simulation results. During stroke height setting, the 3rd stage will be observed by the operator for perfect stroke of serration. According to design, forming requirements for grooving and flatting operation will be confirm by the stroke setting for serration operation.

Springs are provided only in first two stages to maintaining the required force [8]. Analytically, net amount of force essential for all steps is 95484.7 N.

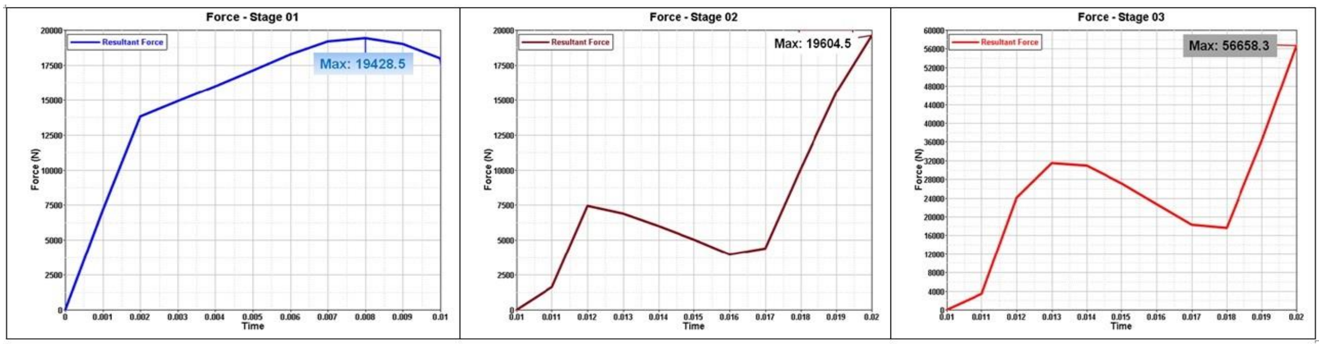

Fig. 15. Force observed after each stage

5. EXPERIMENTATION DETAILS

As per the designed calculation and simulation results, various components of combination tool were developed in the tool room. The designed tool was fabricated by assembly of all the components and fixed on the available press as shown in Figure 16. As per required force mentioned in section 4.2, the press of capacity greater than or equals to 10-ton would be sufficient to perform the experimental work. The experimentation was conducted in automotive component industry.

Fig 16. New fabricated tool

The combination tool is having larger bed size, which will not fit on the press of 10-ton capacity. The press having larger bed size was used to carry out required operation.
The 'SEYI SN1 110' press machine is used to carry out the experimentation. Before the actual experimentation huge numbers of trials were conducted on the same press. All required three operations were performed in single stroke with only one operator for complete cycle.

6. RESULTS AND EXPERIMENTAL VALIDATION

Results found from the trials using new combination tool to manufacture connecting rod are compared with the old tool related to cycle time. From the Table 2, it is seen that cycle time required for performing all three operations on connecting rod reduces up to 22.86 seconds. From comparison with the previous tool more than 50% decrease in cycle time is observed. This drop in total cycle time is because of minimum operation time, minimum handling of material (loading and unloading of separate die) and reduction in component rejection.

Table 2. Comparison of cycle time

Sr. No.	Process/ Operation	Loading Time/ Batch (hr)	Cycle Time (sec)	No. of Operators	No. of Helpers
Old Tool					
1	Grooving	0.5	8.73	1	1
2	Flattening	0.5	8.73	1	1
3	Serration	0.5	8.73	1	1
New Tool					
1	Combination tool	0.5	3.33	1	NA
Total reduction		**1.0**	**22.86**	**2**	**3**

Additionally, the manpower required for the process is also reduced. Tiredness of operator at rework location minimizes by using new combination tool, as various defects occurred in the component are reduced. Huge reduction in rejection is obtained using this combination tool. This also leads to improve the productivity of the firm as well as it shows significant optimization of the process. Figure 17 illustrated the speedy production with the help of new combination tool. The tool is experimentally validated in an industrial unit using the results obtained with FE simulation. This shows remarkable improvement in the reduction of cycle time through process optimization. Thus, the optimization in the process observed due to combining the three operations in single one with the aid of FE simulation.

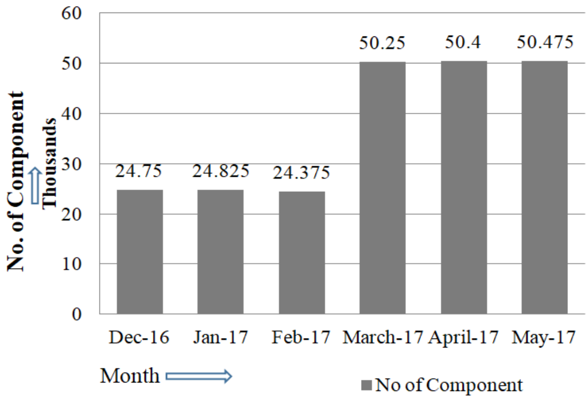

Fig. 17. Production improvement

7. CONCLUSIONS

This research work is centered on process improvement by designing a new combination tool and simulating the forming process to accomplish three different operations concurrently for replacement of existing tools. The use of metal forming simulation leads to a significant reduction in both cost and time compared with the use of trial tools, as the simulation is very effective to quickly test new ideas which may be essential when designing the tools for forming complex parts. In the present study, the analytically calculated forces and forming forces predicted by the simulations by using LS-Dyna are compared and found almost same. The final formed shape of the part is an important aspect in the validation for these forming simulations. The validation of design is performed experimentally. It has been noticed that performing three operations concurrently with nominal material handling has reduced the cycle duration by more than 50% compared to earlier conventional tools.
Similar kind of design trend can be applied to develop a combine tool for multiple operations. FE simulation is the best applied tool to analyze and forecast the results before actual manufacturing of tool. The most important factor which needs to be considered by designer during the design stage is the calculation of force and deflection.

8. REFERENCES

1. Gantar, G., Pepelnjak, T. and Kuzman, K. (2002). *Optimization of sheet metal forming processes by the use of numerical simulations.* Journal of Materials Processing Technology, **130-131**, pp. 54-59.
2. Ingarao, G. and Di Lorenzo, R. (2010). *A new progressive design methodology for complex sheet metal stamping operations: Coupling spatially differentiated restraining forces approach and multi-objective optimization.* Computers & Structures, **88**(9-10), pp. 625-638.

3. Andersson, A. (2001). *Information exchange within the area of tool design and sheet-metal-forming simulations.* Journal of Engineering Design, **12**(4), pp. 283-291.
4. Andersson, A. (2004). *Comparison of sheet-metal-forming simulation and try-out tools in the design of a forming tool.* Journal of Engineering Design, **15**(6), pp. 551-561.
5. Chinesta, F. and Cueto, E. (2007). *Advances in Material Forming.* Paris: Springer Paris, pp. 11-21.
6. Tisza, M. (2004). *Numerical modelling and simulation in sheet metal forming.* Journal of Materials Processing Technology, **151**(1-3), pp. 58-62.
7. Chang, K. (2014). *Product manufacturing and cost estimating using CAD/CAE.* Estados Unidos: Elsevier Inc., pp. 133-190.
8. Chavan, H. and Wani, V. (2018). *Design of combination tool for an automotive component with process optimization in metal forming.* International Journal on Interactive Design and Manufacturing **13**, pp. 401–412.
9. Chavan, H. and Wani, V. (2019). *Evaluation of forming parameters affecting the grooving process for automotive connecting rod: an experimental and statistical approach.* International Journal of Productivity and Quality Management, **27**(3), pp. 249-275.
10. AZoM.com. (2018). *O1 Tool Steel - Oil-Hardening Cold-Work Steel (UNS T31501).* [online] Available at: http://www.azom.com/article.aspx?ArticleID=6229 Accessed on: 15 Nov. 2016.
11. Ismail, H., Chen, S. and Hon, K. (1996). *Feature-based design of progressive press tools.* International Journal of Machine Tools and Manufacture, **36**(3), pp. 367-378.
12. Rao, P. (2013). *Manufacturing technology.* New Delhi: Mc Graw Hill.
13. Hiller, N. (2014). *Basic Theory of Structures.* Elsevier Science.
14. Choi, K., Lee, M. and Kim, H. (2013). *Sheet metal forming simulation considering die deformation.* International Journal of Automotive Technology, **14**(6), pp. 935-940.
15. Del Prete, A., Primo, T. and Strano, M. (2010). *The use of FEA packages in the simulation of a drawing operation with springback, in the presence of random uncertainty.* Finite Elements in Analysis and Design, **46**(7), pp. 527-534.
16. Lin, B. and Kuo, C. (2006). *Application of an integrated CAD/CAE/CAM system for stamping dies for automobiles.* The International Journal of Advanced Manufacturing Technology, **35**(9-10), pp. 1000-1013.
17. Fu, M., Yong, M., Tong, K. and Muramatsu, T. (2006). *A methodology for evaluation of metal forming system design and performance via CAE simulation.* International Journal of Production Research**, 44**(6), pp. 1075-1092.
18. Maker, B. and Zhu, X. (2001). *Input Parameters for Springback Simulation Using LS-DYNA.* [ebook] Livermore Software Technology Corporation, 1-11. Availableat:https://www.dynalook.com/Personally/springback_maker_zhu.pdf, Accessed on: 6 Jun. 2018.
19. Makinouchi, A. (1996). *Sheet metal forming simulation in industry.* Journal of Materials Processing Technology, **60**(1-4), pp. 19-26.
20. Ahmed, G., Ahmed, H., Mohiuddin, M. and Sajid, S. (2014). *Experimental Evaluation of Springback in Mild Steel and its Validation Using LS-DYNA.* Procedia Materials Science, **6**, pp. 1376-1385.
21. Naranjo, J., Miguel, V., Martínez-Martínez, A., Gómez-López, L., Manjabacas, M. and Coello, J. (2015). *Analysis and Simulation of Single Point Incremental Forming by ANSYS®.* Procedia Engineering, **132**, pp. 1104-1111.
22. Bauer, F., Werber, A. and Merklein, M. (2017). *Investigation of a process simulation method for flexible clamping of sheet metal parts.* Procedia Engineering, **207**, pp. 1599-1604.

Received: February 15, 2021 / Accepted: June 15, 2021 / Paper available online: June 20, 2021